Cathepsin S Controls Angiogenesis and Tumor Growth via Matrix-derived Angiogenic Factors

THE JOURNAL OF BIOLOGICAL CHEMISTRY VOL. 281, NO. 9, pp. 6020–6029, March 3, 2006

Cathepsin S Controls Angiogenesis and Tumor Growth via Matrix-derived Angiogenic Factors*

Received for publication, August 18, 2005, and in revised form, December 16, 2005 Published, JBC Papers in Press, December 19, 2005, DOI 10.1074/jbc.M509134200

Bing Wang[‡], Jiusong Sun[‡], Shiro Kitamoto[‡], Min Yang[‡§], Anders Grubb[¶], Harold A. Chapman[‖], Raghu Kalluri[**], and Guo-Ping Shi[‡1]

*From the [‡]Department of Medicine, Brigham and Women's Hospital and Harvard Medical School, Boston, Massachusetts 02115, the [§]Department of Nephrology, Nanfang Hospital, Southern Medical University, Guangzhou 510515, China, the [¶]Department of Clinical Chemistry, University Hospital, S-22185 Lund, Sweden, the [‖]Department of Medicine, University of California, San Francisco, California 94143, and the **Center for Matrix Biology, Beth Israel Deaconess Medical Center and Harvard Medical School, Boston, Massachusetts 02215*

The cysteine protease cathepsin S is highly expressed in malignant tissues. By using a mouse model of multistage murine pancreatic islet cell carcinogenesis in which cysteine cathepsin activity has been functionally implicated, we demonstrated that selective cathepsin S deficiency impaired angiogenesis and tumor cell proliferation, thereby impairing angiogenic islet formation and the growth of solid tumors, whereas the absence of its endogenous inhibitor cystatin C resulted in opposite phenotypes. Although mitogenic vascular endothelial growth factor, transforming growth factor-β1, and the anti-angiogenic endostatin levels in either serum or carcinoma tissue extracts did not change in cathepsin S- or cystatin C-null mice, tumor tissue basic fibroblast growth factor and serum type 1 insulin growth factor levels were higher in cystatin C-null mice, and serum type 1 insulin growth factor levels were also increased in cathepsin S-null mice. Furthermore, cathepsin S affected the production of type IV collagen-derived anti-angiogenic peptides and the generation of bioactive pro-angiogenic γ2 fragments from laminin-5, revealing a functional role for cathepsin S in angiogenesis and neoplastic progression.

Angiogenesis, the development of the microvasculature, is an essential process occurring under many pathological and physiological circumstances and depends on tightly controlled interactions between cells and extracellular matrix (ECM)[2] mediated by integral membrane proteins. These include integrins, which provide a link between ECM and the cytoskeleton, and extracellular proteases and their inhibitors, which mediate focal degradation of ECM components (1, 2), generate cell growth factors (3), and produce angiogenic regulatory factors (4).

Lysosomal cysteine protease cathepsins have been shown to be highly expressed in human and murine tumors (5), where angiogenesis plays essential roles. Interruption of their expression either by antisense RNA (6) or RNA interference (7, 8) reduced tumor cell invasion, angiogenesis, and tumor growth. A recent study also demonstrated that inhibition of the activities of cysteine proteases with a broad inhibitor reduced angiogenesis and growth of pancreatic β-cell islet carcinoma in mice with an SV40 T antigen (Tag) transgene driven by the rat insulin II promoter (RIP1-Tag2) (9). Administration of JPM-ethyl ester (10), which affects all activities of cysteinyl cathepsins, significantly diminished the angiogenic switch, tumor burden, and tumor cell proliferation (11). However, many important questions are still unanswered; for example, which cathepsin(s) is the most important and by what mechanisms do these cysteinyl cathepsins affect tumor progression? Earlier studies suggested the importance of cathepsin (Cat) B in tumor angiogenesis and growth (6–8). However, additional studies also demonstrated constitutive expression of Cat B in several cell types or tissues (12, 13). Therefore, cathepsins other than Cat B may also be involved in angiogenesis, tumor growth, cell proliferation, and metastasis. We tested this hypothesis in our previous study with Cat S-deficient endothelial cells *in vitro*. Inhibition of Cat S activity or the absence of Cat S expression reduced microvessel formation in Matrigel (14). Here we introduced mutant alleles of Cat S or its inhibitor cystatin (Cyst) C into the RIP1-Tag2 transgenic tumor model, in which the angiogenic switch is a key step in islet cell carcinogenesis, to test whether the absence of Cat S or Cyst C expression affected tumor growth and, if so, to investigate the underlying molecular mechanisms.

EXPERIMENTAL PROCEDURES

Generation of RIP1-Tag2/Cat $S^{-/-}$ and RIP1-Tag2/Cyst $C^{-/-}$ Mice—RIP1-Tag2 transgenic mice (in C57/Bl6 background) (11) were cross-bred with Cat $S^{-/-}$ mice (in C57/Bl6 background), and the resulting RIP1-Tag2/Cat $S^{+/-}$ mice were backcrossed to Cat $S^{-/-}$ or wild-type mice to generate both RIP1-Tag2/Cat $S^{-/-}$ and RIP1-Tag2/Cat $S^{+/+}$ mice. Cyst $C^{-/-}$ (mixed background) (15) mice were also cross-bred with RIP1-Tag2 transgenic mice. The resulting RIP1-Tag2/Cyst $C^{+/-}$ mice were used as breeding pairs to generate RIP1-Tag2/Cyst $C^{+/+}$ and RIP1-Tag2/Cyst $C^{-/-}$ littermates. When mice were 10.5 weeks old, serum was collected, and pancreatic angiogenic islets were harvested, counted, and optimal cutting temperature compound (OCT)-embedded. At 12.5 weeks, mouse serum samples were collected, islet cell carcinomas were harvested, and tumors were measured according to the formula (volume = 0.52 × (width)^2 × length in mm^3) and embedded in OCT for tissue-section staining or protein extraction into pH 7.2 lysis buffer (150 mM NaCl, 1% Triton X-100, 0.015 M $CaCl_2$, 0.1% SDS, 0.5% sodium deoxycholate) for MMP zymogram, ELISA, and immunoblot analysis or pH 5.5 lysis buffer (1 mM EDTA, 0.05% Triton X-100, 20 mM sodium acetate) for cysteine protease active-site labeling.

Immunohistochemistry—Serial cryostat sections (6 μm) of pancreatic islet cell carcinoma were fixed in acetone (−20 °C, 10 min) and

* This work was supported by National Institutes of Health Grants HL60942, HL67283 (to G. P. S.), HL48621 (to H. A. C.), and DK62987 (to R. K.). The costs of publication of this article were defrayed in part by the payment of page charges. This article must therefore be hereby marked "*advertisement*" in accordance with 18 U.S.C. Section 1734 solely to indicate this fact.

[1] To whom correspondence should be addressed: Cardiovascular Medicine, NRB-7, 77 Ave. Louis Pasteur, Boston, MA 02115. Tel.: 617-525-4358; Fax: 617-525-4380; E-mail: gshi@rics.bwh.harvard.edu.

[2] The abbreviations used are: ECM, extracellular matrix; Cat, cathepsin; Cyst C, Cystatin C; RIP1-Tag2, rat insulin II promoter driven T antigen; MMPs, matrix metalloproteinases; VEGF, vascular endothelial growth factor; bFGF, basic fibroblast growth factor; IGF-1, type I insulin growth factor; TGF-β1, transforming growth factor-β1; ELISA, enzyme-linked immunosorbent assay; PBS, phosphate-buffered saline.

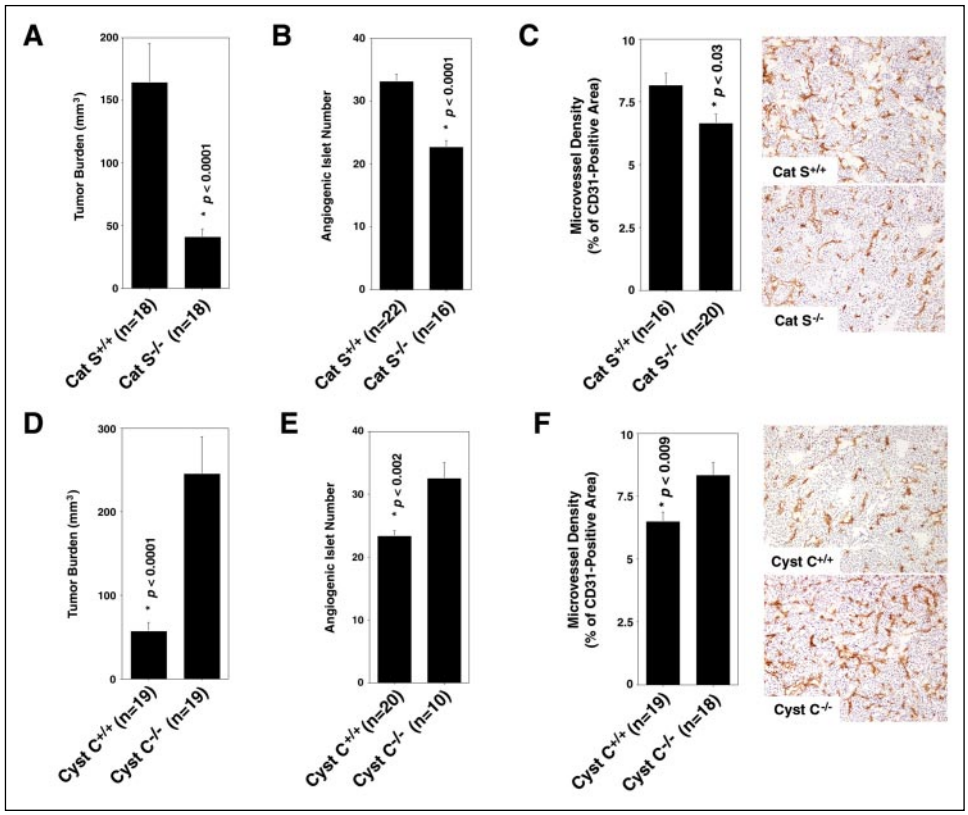

FIGURE 1. **Expression of Cat S and Cyst C affects angiogenesis and tumor growth.** Deficiency of Cat S reduced tumor burden at 12.5 weeks (*A*), angiogenic islet numbers at 10.5 weeks (*B*), and tumor microvessel density (*C*) in RIP1-Tag2 mice. *Right panels* are representative immunostaining of CD31. In contrast, absence of Cyst C increased tumor sizes (*D*), angiogenic islet numbers (*E*), and tumor microvessel density at 12.5 weeks (*F*) in the same RIP1-Tag2 transgenic mice. Representative CD31 staining is also shown in the *right panels*.

stained by the avidin-biotin-peroxidase method (ABC kit, Vector Laboratories). After peroxidase activity was limited with 0.3% hydrogen peroxide and nonspecific binding of primary antibody with 5% species-appropriate normal serum, sections were incubated with primary antibodies diluted in PBS overnight at 4 °C. Incubation with secondary antibodies for 30 min was followed by incubation with the avidin-biotin complex conjugated with horseradish peroxidase for another 30 min. The reaction was visualized with 3,3′-diaminobenzidine (Vector Laboratories) followed by counterstaining with Gill's hematoxylin solution (Fisher) or methyl green (DAKO). The antibodies used were rat anti-mouse CD31 (1:800; Pharmingen), rabbit anti-human Ki67 (1:1000; Novacastra Laboratories, UK), and rabbit anti-mouse canstatin, tumstatin, and arresten (1:500) (16–18).

Microvessel density of each tumor was determined by measuring the pixel area of CD31-positive staining in five random areas using the image analysis software Image-Pro Plus as described previously (15, 19). A total of 16–20 tumors per group were selected, and data were presented as percentage of CD31-positive areas (mean ± S.E.), CD31-positive area *versus* image area (×100). The percentage of Ki67-positive cells was determined by scanning rabbit anti-human Ki67 antibody-stained slides and choosing five random areas per tumor to count both Ki67-positive and total cell numbers, with data presented as mean ± S.E. of the Ki67-positive cell percentage.

Percentages of positive areas of canstatin, arresten, and tumstatin were determined by capturing five random areas of each slide (×100), and positive staining on each image was quantified using the same image analysis software Image-Pro Plus as we described previously (15), and data were presented as mean ± S.E.

Cysteine Protease Active-site Labeling and MMP Zymography—Tumor tissue cysteine protease and MMP activities were determined by pulverizing tumor tissues and extracting into pH 5.5 buffer (cysteine proteases) or pH 7.2 buffer (MMPs). Protein concentrations were determined with the *Dc* protein assay kit (Bio-Rad). Cysteine protease activities were measured by labeling equal amounts of protein (100 μg) of each sample with ^{125}I-JPM at 37 °C for 1 h as described previously (15) followed by separation on 14% SDS-PAGE. MMP activities were assessed by separating 2 μg of protein from each sample on 10% SDS-PAGE containing 1 mg/ml gelatin and then visualizing active MMP-9 and MMP-2 signals by a protocol described previously (20).

Blood Glucose Measurement—Commercial blood glucose strips were purchased from Home Diagnosis Inc. (Ft. Lauderdale, FL). One drop of blood was applied to the strip, and the glucose was measured directly on the supplied blood glucose meter.

ELISA—VEGF (R & D Systems, Minneapolis, MN), bFGF (R & D Systems), IGF-1 (Immunodiagnostic Systems, UK), TGF-β1 (Biosources, Camarillo, CA), and endostatin (Cytimmune Sciences, Rockville, MD) in tumor tissue lysates and serum were determined with commercially available ELISA kits according to the manufacturers' protocols. In brief, tissue lysates, sera, and known concentrations of recombinant growth factors, as internal standards, were added to the wells of 96-well microtiter plates, which were precoated with capturing antibodies to the specific growth factor being assessed. After a 2-h incubation at room temperature, the plate was washed four times, and a biotinylated detecting antibody to the growth factor was added and incubated for another hour followed by 30 min of incubation with streptavidin-horseradish peroxidase conjugate. The plate was then washed four times, and a premixed TMB substrate solution was added. The plate was developed at room temperature in the dark for 30 min before the reaction was stopped. The absorbance of each well was measured at 450 nm with an ELISA reader.

Immunoblot Analysis—Equal amounts of tumor extracts (40 μg) or equal volumes of serum (2 μl) from each mouse were separated on 8 (to detect laminin-5 γ2 chains) or 14% (to detect canstatin) SDS-PAGE and

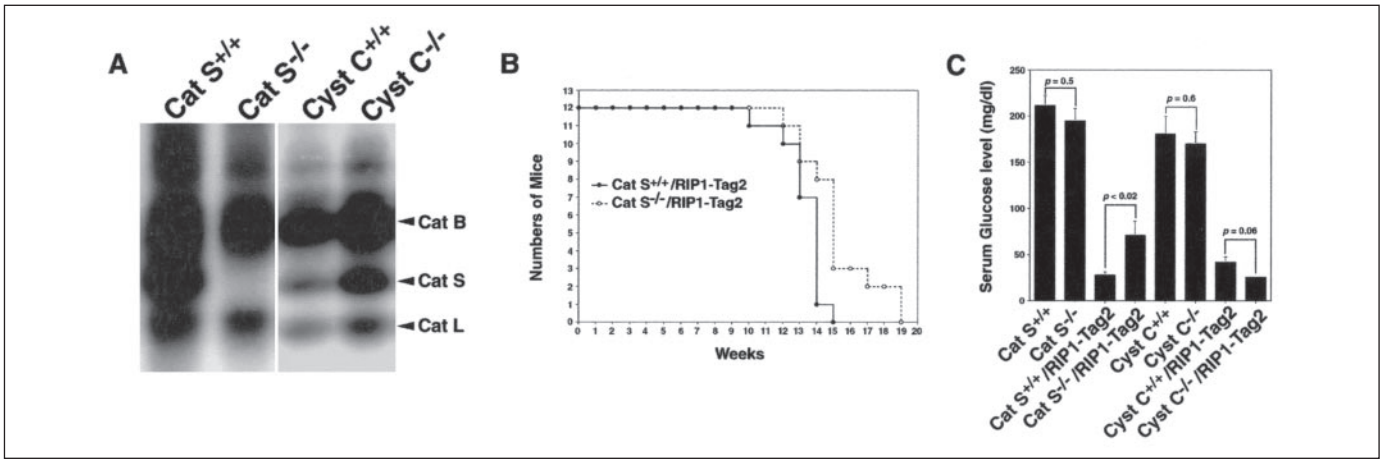

FIGURE 2. **Impact of Cat S and Cyst C expression on the expression of other cysteine proteases, animal life span, and hypoglycemia.** *A,* RIP1-Tag2 tumor extracts from 12.5-week-old different knock-out mice were labeled with ^{3}H-JPM and separated on 14% SDS-PAGE. Different active cathepsins are indicated by *arrowheads. B,* mouse life span was monitored and recorded weekly. Cat S deficiency extended the life spans of RIP1-Tag2 mice by 2 weeks on average (15.2 ± 0.6 *versus* 13.3 ± 0.3, $p < 0.05$). *C,* serum glucose levels were measured at 10.5 weeks in each group of mice. All RIP1-Tag2 transgenic mice had decreased serum glucose levels, and Cat S deficiency significantly increased serum glucose levels.

blotted onto a polyvinylidene difluoride membrane. Primary antibodies included rabbit anti-mouse canstatin (1:1000) (16) and mouse laminin-5 γ2 chain monoclonal antibody (γ2LE4-6; 1:1000) (21). A β-actin immunoblot was performed as a loading control for tumor extract proteins (1:5000; Sigma).

Canstatin and Arresten Degradation by Recombinant Cat S—One microgram of purified recombinant murine canstatin (16) or arresten (17) was incubated with various amounts of recombinant human Cat S (0, 0.1, 1, and 10 nM) in a pH 5.5 reaction buffer containing 50 mM sodium acetate, 0.1% Triton, and 6 mM dithiothreitol for 1 h at 37 °C. Reaction mixtures were separated on a 10% SDS-PAGE followed with immunoblot detection with rabbit polyclonal antibodies against murine canstatin and arresten (1:1000).

Laminin-5 Degradation by Recombinant Human Cat S—Human epidermoid carcinoma A431 cells were cultured in 150-mm cell culture dishes in Dulbecco's modified Eagle's medium with 10% fetal calf serum until confluent. Cells were then lysed and washed in 1× PBS containing 0.5% Triton four times for 10 min at 4 °C as described to remove intracellular proteins (22). Cell skeletons were prepared by washing cells with 2 M urea in 1 M NaCl for 10 min at 4 °C followed by another wash with 1× PBS. Cell skeleton preparations were collected into 1.5-ml Eppendorf tubes and then incubated with or without recombinant human Cat S at different concentrations (60, 3, 0.15, and 0.0075 nM) in a pH 5.5 reaction buffer for 1 h at 37 °C. Reaction mixtures were separated directly on 8% SDS-PAGE for immunoblot analysis with human laminin-5 monoclonal antibody 19562 (1:1000; Chemicon).

Laminin-5 degradation by Cat S was further examined by culturing the A431 cells on 6-well plates. After confluent cells were lysed and washed with 1× PBS, 0.5% Triton, 2 mM urea, 1 M NaCl, and 1× PBS, primary cultured mouse endothelial cells (1×10^6/well) from Cat $S^{-/-}$ and wild-type mice were seeded onto each well followed by an overnight incubation. Culture media and cell lysates, which contain the whole endothelial cells and residual A431 matrix protein, were collected. Equal amounts of lysate (40 μg/well) and culture media (concentrates from 100 μl of culture media) were separated on 8% SDS-PAGE followed by immunoblot staining with human laminin-5 monoclonal antibodies (1:1000).

Purification of Cat S-generated Laminin-5 γ2 Fragments and Aortic Ring Assay—A431 cell skeleton protein preparations were digested with recombinant Cat S (0.5, 5, and 30 nM) at 37 °C for 1 h. Reactions were terminated with 10 nM Cat S-selective inhibitor *N*-morpholinurea-leucine-homophenylalanine-vinylsulfone-phenyl (23) and neutralized with 0.5 M Tris·HCl, pH 10.2. After removal of nondigested precipitates, supernatant was incubated with AminoLink® Plus coupling gel (Pierce) coupled with human laminin-5 monoclonal antibody. After overnight incubation at 4 °C, the affinity gel was washed and eluted into fractions. The peptide purity in each fraction was examined on an 8% SDS-polyacrylamide gel followed by silver staining, and peptide specificity was verified with an immunoblot analysis using human laminin-5 monoclonal antibody (21). Protein concentration of each purified peptide was determined with the Bio-Rad *Dc* protein assay kit according to the manufacturer's instructions.

The bioactivity of purified laminin-5 γ2 fragments was examined with an aortic ring assay as described previously (24). Briefly, a 96-well plate was covered with 50 μl of Matrigel (BD Biosciences). A 1-mm-long mouse aortic ring was laid on the top of the Matrigel and covered with another 100 μl of Matrigel. After 30 min of solidification, 100 μl of Dulbecco's modified Eagle's medium without fetal calf serum, with or without purified laminin-5 γ2 fragments, was added to each well to a final concentration of 10 ng/ml. The combination of bFGF (10 ng/ml) and interferon-γ (500 units/ml) was used as a positive control (24). After 10 days of culture, the gels were photographed, and the endothelial outgrowth was analyzed by manually circulating and computing square pixels and quantified by Image-Pro Plus software. Data were presented as mean area ± S.E. (mm^2). p values <0.05 were considered significant (Mann-Whitney test).

RESULTS

Deficiency of Cat S and Its Inhibitor Cyst C in Mice Altered Angiogenesis, Tumor Growth, and Life Span—RIP1-Tag2 transgenic mice (9) develop pancreatic islet cell carcinoma over time in stages. At the age of 12–14 weeks, well established solid tumors can be detected. Beginning at 10.5 weeks of age, nascent solid tumors form by progressing from a dysplastic stage called angiogenic islets, only a small fraction of which ultimately progress into mature carcinomas. This model provides a useful system for assessing the contribution of proteases and protease inhibitors to angiogenesis and tumor growth. To examine whether cysteine protease Cat S participates in these pathologic events, we generated Cat S-deficient (Cat $S^{-/-}$) RIP1-Tag2 mice (in C57/BL6 background). Relative to RIP1-Tag2/Cat $S^{+/+}$ mice (wild type for Cat S), RIP1-Tag2/Cat $S^{-/-}$ mice developed much smaller tumors at 12.5

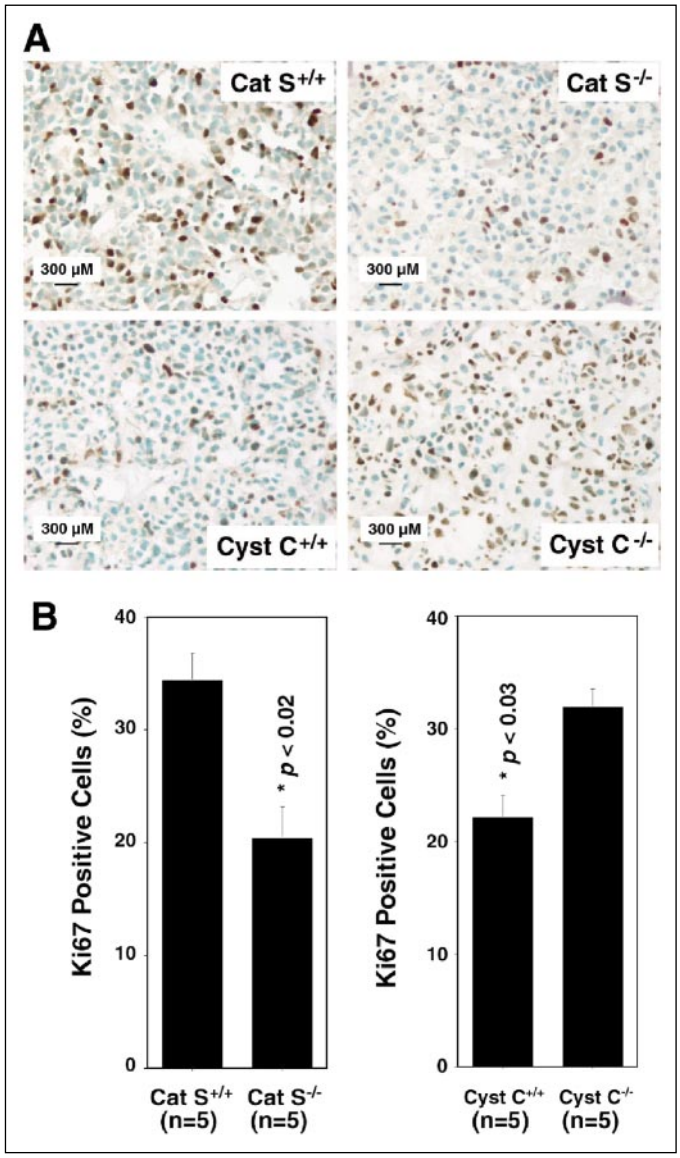

FIGURE 3. **Cat S and Cyst C expression regulates tumor cell proliferation.** *A,* sections of RIP1-Tag2 tumors from different knock-out mice (12.5 weeks) were stained with Ki67. *Brown* cells indicate Ki67-positive proliferating tumor cells. *B,* statistic analysis (Mann-Whitney test) demonstrated reduced tumor cell proliferation in Cat $S^{-/-}$ tumors but increased hyperplasia in Cyst $C^{-/-}$ mice.

weeks of age (Fig. 1*A*) and significantly fewer angiogenic islets at age 10.5 weeks (Fig. 1*B*). Immunostaining for endothelial cells (CD31) demonstrated reduced microvessel density in tumors from RIP1-Tag2/Cat $S^{-/-}$ mice (Fig. 1*C*).

Cyst C is an endogenous inhibitor of cysteine proteases, with highest inhibitory competency for Cat S (25). A previous study reported that the absence of Cyst C increased the activities of cysteinyl cathepsins in tissues under inflammatory conditions (15). To examine the impact of Cyst C and to assess further the importance of Cat S and other cysteine cathepsins in angiogenesis and tumor growth (given that six cysteine cathepsins are up-regulated in this model; see Ref. 11), we generated Cyst C-deficient (Cyst $C^{-/-}$) RIP1-Tag2 mice (C57/BL6/129S mixed background). Relative to their RIP1-Tag2/Cyst $C^{+/+}$ littermates, RIP1-Tag2/Cyst $C^{-/-}$ mice developed much larger islet cell carcinomas at age 12.5 weeks (Fig. 1*D*) and significantly more angiogenic islets at age 10.5 weeks (Fig. 1*E*). Consistently, the density of CD31-positive microvessels from the tumors was much higher in the RIP1-Tag2/Cyst $C^{-/-}$ mice (Fig. 1*F*).

To examine whether the lack of Cat S or Cyst C in RIP1-Tag2 mice affected other cathepsins or even MMPs activity that might contribute to the phenotypes in Fig. 1, we labeled tumor extracts from the RIP1-Tag2/Cat $S^{-/-}$ and RIP1-Tag2/Cyst $C^{-/-}$ mice and their corresponding wild-type controls by ^{125}I-JPM, which labels only active cysteine proteases (23), and we then performed a gelatin zymogram assay to assess the relative MMP-2 and MMP-9 activity in these tissues. We detected no changes in any cathepsins other than a difference in Cat S expression between RIP1-Tag2/Cat $S^{+/+}$ and RIP1-Tag2/Cat $S^{-/-}$ mice (Fig. 2*A*). In contrast, we detected more ^{125}I-JPM-labeled cathepsin signals, especially Cat S and Cat L, in tumor extracts from RIP1-Tag2/Cyst $C^{-/-}$ mice than in those from RIP1-Tag2/Cyst $C^{+/+}$ mice (Fig. 2*A*), although we observed no differences in MMP activity in the presence or absence of Cat S or Cyst C (data not shown). Therefore, altered Cat S activity is evidently one of the factors affecting altered tumor growth and angiogenesis in RIP1-Tag2/Cat $S^{-/-}$ and RIP1-Tag2/Cyst $C^{-/-}$ mice (Fig. 1).

Because of the absence of Cat S-reduced tumor growth, we asked whether such alteration might prolong the life span of tumor-bearing mice. RIP1-Tag2 mice receiving a chow diet are known to die of hypoglycemia any time after 12 weeks of age (9). We monitored 12 mice from each group (RIP1-Tag2/Cat $S^{+/+}$ and RIP1-Tag2/Cat $S^{-/-}$) and noted that Cat S deficiency prolonged the life span of RIP1-Tag2 mice by an average of 2 weeks (13.3 ± 0.3 *versus* 15.2 ± 0.6, $p < 0.05$) (Mann-Whitney test). Consistent with earlier findings (9), mice bearing the RIP1-Tag2 transgene demonstrated significantly lower serum glucose levels than their counterparts without the transgene (Fig. 2*C*). Among all RIP1-Tag2 mice tested, RIP1-Tag2/Cat $S^{-/-}$ mice showed higher serum glucose levels than RIP1-Tag2/Cat $S^{+/+}$ mice (Fig. 2*C*), which may also contribute to the prolonged life span observed in RIP1-Tag2/Cat $S^{-/-}$ mice. Consistent with insignificant changes in serum glucose levels between RIP1-Tag2/Cyst $C^{+/+}$ and RIP1-Tag2/Cyst $C^{-/-}$ mice, we detected no significant differences in life span (15.7 ± 0.8 *versus* 16.7 ± 0.7, $p = 0.3$), although both groups lived significantly longer than RIP1-Tag2/Cat $S^{+/+}$ mice did, likely because of the genetic background differences.

Cat S Activity on Tumor Cell Proliferation, Pro-angiogenic Growth Factors, and Anti-angiogenic Endostatin—Inhibition of cysteinyl cathepsins by JPM-ethyl ester has been found to impair tumor cell proliferation in the RIP1-Tag2 islet cell carcinoma model (11). By using this same tumor model with the absence of Cat S expression, we observed a similar phenotype. Tumor cell proliferation was reduced in RIP1-Tag2/Cat $S^{-/-}$ tumors, with significant reduction of the percentage of Ki67-positive cells (Fig. 3, *A* and *B*). In contrast, the percentage of Ki67-positive cells was increased in RIP1-Tag2/Cyst $C^{-/-}$ tumors, most likely because of enhanced cysteinyl cathepsin activity and loss of Cyst C activity in antagonizing cell proliferation (26, 27) (Fig. 3, *A* and *B*). Thus, Cat S activity is functionally involved in regulating tumor cell proliferation in a nonredundant fashion, given that five other cysteine cathepsins are expressed (11). Despite the fact that Cat S deficiency impairs the neoplastic phenotype, we cannot exclude the possibility that these other cathepsins are also contributing to tumor cell proliferation.

Cellular growth factors play essential roles in regulating cell migration, proliferation, protease expression, and matrix remodeling, angiogenesis, tumor growth, and metastasis. Multiple studies have demonstrated that proteases participate in the release of growth factors from the extracellular matrix and basement membranes, either by converting them from their latent forms or degrading their associated inhibitors (9,

TABLE 1

Growth factor and endostatin levels in mice lacking cathepsin S or cystatin C

Unless indicated otherwise, the nonparametric Mann-Whitney test showed $p > 0.05$.

Genotypes (n)	VEGF (pg/ml)		bFGF (pg/ml)		IGF-1 (ng/ml)		TGF-β1 (pg/ml)		Endostatin (ng/ml)	
	Serum	Extract	Serum	Extract	Serum	Extract	Serum	Extract	Serum	Extract
Cat $S^{+/+}$	54.2±5.3 (n=14)	918.2±18.1 (n=6)	38.9±6.5 (n=14)	448.4±62.9 (n=14)	311.2±28.1 (n=14)	12.0±11.5 (n=6)	424.5±18.5 (n=13)	UD** (n=10)	13.9±1.0 (n=14)	34.4±24.6 (n=6)
Cat $S^{-/-}$	58.1±9.7 (n=14)	913.4±14.3 (n=7)	35.1±7.1 (n=14)	880.8±153.8 (n=14) p=0.002	321.1±30.6 (n=14)	8.9±5.2 (n=7)	429.7±13.9 (n=14)	UD (n=10)	13.9±0.7 (n=14)	20.8±15.2 (n=7)
Cyst $C^{+/+}$	64.2±6.7 (n=14)	889.4±41.5 (n=6)	32.8±6.1 (n=14)	746.1±74.8 (n=13)	312.6±29.7 (n=13)	17.1±7.4 (n=6)	421.3±14.5 (n=11)	UD (n=10)	12.3±0.6 (n=10)	5.7±1.5 (n=6)
Cyst $C^{-/-}$	60.2±5.6 (n=14)	885.7±24.1 (n=5)	35.5±6.6 (n=14)	1383.6±117.0 (n=12) p=0.0004	601.1±171.7 (n=12) p=0.02	19.2±11.3 (n=5)	457.3±8.7 (n=11)	UD (n=10)	12.1±0.9 (n=14)	5.6±1.7 (n=5)

** UD indicates undetectable.

28–31). We therefore asked whether a deficiency of Cat S or an increase in the expression of cysteinyl cathepsins because of the lack of Cyst C had any impact on levels of angiogenesis-associated growth factors. Such effects might explain the phenotypes shown in Figs. 1 and 3. We measured circulating VEGF, bFGF, IGF-I, and TGF-β1 in mouse tumor tissue extracts and serum samples with ELISA (Table 1). Although the absence of Cat S or Cyst C did not show a significant impact on the levels of VEGF and TGF-β1, the absence of Cyst C increased bFGF levels in the tumor extract and IGF levels in the serum, which may partially account for increased tumor cell proliferation (Fig. 3) and tumor growth (Fig. 1, *D–F*) in these mice. However, increased tumor tissue bFGF was also detected in Cat $S^{-/-}$ mice, although accompanied with reduced tumor cell proliferation (Fig. 3) and tumor growth (Fig. 1, *A–C*), suggesting involvement of additional mechanisms.

Endostatin is a proteolytic fragment of type XVIII collagen generated by several proteases *in vitro*, including cysteinyl cathepsins (32, 33), serine elastases (34), and MMPs (35). It is possible that Cat S or other cathepsins affect the circulating levels of this anti-angiogenic peptide in live animals. However, by using an endostatin ELISA, we detected no significant differences in endostatin levels in mouse sera or tumor extracts in the presence or absence of Cat S or Cyst C expression (Table 1), suggesting a minor effect of Cat S in endostatin production *in vivo*, although the contribution of other cathepsins in collagen XVIII degradation and endostatin production may require further investigation.

Cat S Regulated the Levels of Type IV Collagen-derived Anti-angiogenic Peptides—Canstatin, arresten, and tumstatin are three novel anti-angiogenic peptides recently identified from the processing products of the basement membrane type IV collagen (16–18). Both *in vitro* and *in vivo*, these peptides demonstrably inhibit endothelial cell proliferation, angiogenesis, and tumor growth (16–18, 36–38). Although the exact proteases responsible for the generation of canstatin and arresten are unknown, MMP-9 has been shown to be responsible for the production of tumstatin from the α3 chain of type IV collagen (38). We did not detect significant effects of Cat S or Cyst C on endostatin production from type XVIII collagen (Table 1), and we thus asked whether Cat S affected the production of type IV collagen-derived anti-angiogenic peptide. By using an immunostaining technique, we were able to measure quantitatively the differences in the areas positive for canstatin, arresten, and tumstatin in tumor sections from four groups of tumor mice (Fig. 4). We found no statistical differences in the percentage of tumstatin-positive areas of RIP1-Tag2/Cat $S^{+/+}$ and RIP1-Tag2/Cat $S^{-/-}$ mice nor between RIP1-Tag2/Cyst $C^{+/+}$ and RIP1-Tag2/Cyst $C^{-/-}$ mice (Fig. 4*C*), but we noted an enhancement in both canstatin-positive (Fig. 4*A*) and arresten-positive (Fig. 4*B*) areas in RIP1-Tag2/Cat $S^{-/-}$ tumors and a reduction in RIP1-Tag2/Cyst $C^{-/-}$ tumors. These differences suggest the participation of Cat S in the clearance of these anti-angiogenic peptides via either direct degradation of canstatin and arresten or inactivation of proteases responsible for the production of these peptides. To examine this hypothesis, murine canstatin and arresten were digested with recombinant Cat S *in vitro*. Under physiological concentrations (0.1–1 nM; see Ref. 39), Cat S degraded both arresten and canstatin (Fig. 5), as confirmed by immunoblot analysis with their corresponding polyclonal antibodies (16, 17).

Results were similar when tumor tissue extracts or serum samples were used for immunoblot analysis. Levels of canstatin were increased in both the RIP1-Tag2/Cat $S^{-/-}$ tumor extracts (Fig. 6*A*, *left panel*) and serum samples (Fig. 6*B*, *left panel*). In contrast, canstatin immunoreactivity was reduced in tumor extracts (Fig. 6*A*, *right panel*) and serum samples (Fig. 6*B*, *right panel*) from the RIP1-Tag2/Cyst $C^{-/-}$ mice, which showed increased Cat S activity (Fig. 2*A*), further supporting the primary importance of Cat S in regulating the levels of anti-angiogenic peptide, which may contribute to the decrease in angiogenic switching and tumor burden in RIP1-Tag2/Cat $S^{-/-}$ mice (Fig. 1).

Cat S Generated Pro-angiogenic γ2 Fragments from Laminin-5—Like type IV collagen, laminin-5 is a common basement membrane matrix protein composed of three glycoprotein subunits, α3, β3, and γ2, which regulate the adhesion, migration, proliferation, invasion, and morphogenesis of tumor cells via interactions with cell-surface α3β1 and α6β4 integrins (40–42). Such proteins, particularly the γ2 subunits, are preferentially expressed in the cytoplasm of epithelial cancer cells located at the advancing edges of the tumors. Interruptions in laminin-5-integrin interactions block the migration of cancer cells (43). However, proteol-

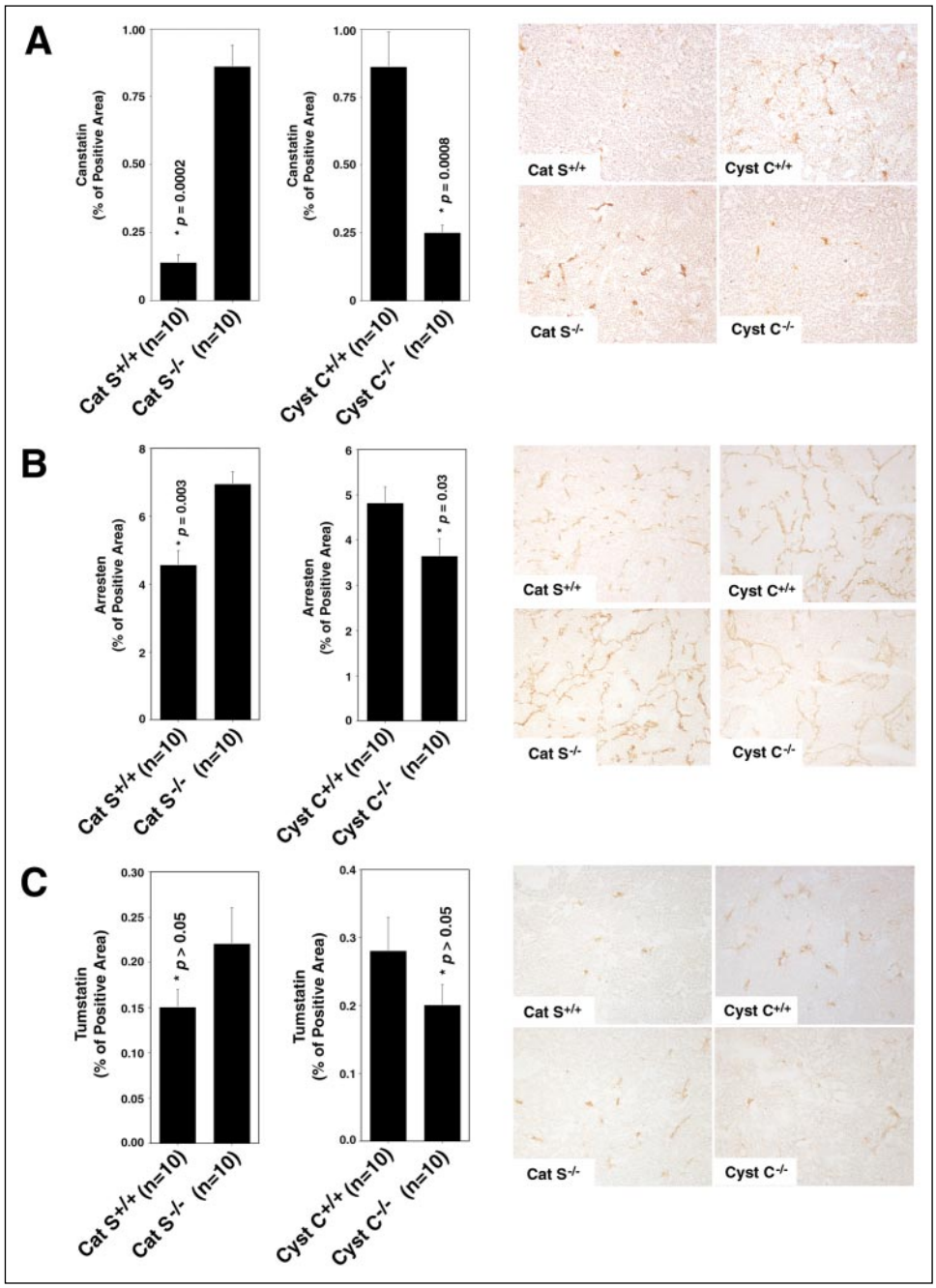

FIGURE 4. **Cat S and Cyst C expression affects tumor levels of anti-angiogenic canstatin, arresten, and tumstatin.** Section of RIP1-Tag2 tumor (12.5 weeks) immunostained with canstatin (*A*), arresten (*B*), and tumstatin (*C*) demonstrated increased percentages of areas of positive immunostaining of these anti-angiogenic peptides in Cat $S^{-/-}$ tumors (*left panels*) but reduced percentages in Cyst $C^{-/-}$ tumors (*middle panels*). *Right panels* are representative immunostaining sections for all three antigens from four groups of mice as indicated.

ysis of laminin-5 and production of its degradation fragments, the γ2-derived fragments, promote cancer cell migration, invasion, and associated vasculogenesis (43, 44). The γ2 subunit of the laminin-5 complex is a 155-kDa polypeptide that can be processed into a 100-kDa pro-angiogenic peptide termed γ2′ and a 30-kDa epidermal growth factor-like motif. Further proteolysis of γ2′ results in another 80-kDa pro-angiogenic γ2χ peptide (45). Therefore, the proteases responsible for the generation of γ2′ and γ2χ peptides become important to angiogenesis and tumor growth. Earlier studies demonstrated the participation of matrix and astacin-like metalloproteinases in the initial γ2 cleavage (46–48). When we used lysates of tumor tissue from the RIP1-Tag2 mice for immunoblot analysis with murine laminin-5 monoclonal antibodies (γ2LE4-6; see Ref. 21), we detected less 80-kDa γ2χ and 100-kDa γ2′ but comparable levels of the 50-kDa γ2 fragment, which we named γ2″, in mice lacking Cat S expression (Fig. 7*A*). In contrast, both γ2′ and γ2χ peptide production were enhanced in tumor extracts from the RIP1-Tag2/Cyst $C^{-/-}$ mice relative to production in RIP1-Tag2/Cyst $C^{+/+}$ mice, presumably due to increased activity of Cat S or other cysteine proteases (Fig. 7*B*), suggesting a participation of Cat S in γ2 processing, possibly contributing to the altered angiogenesis and tumor progression shown in Fig. 1.

We confirmed a direct involvement of Cat S in γ2 processing using recombinant human Cat S and Cat S-deficient mouse endothelial cells. Human laminin-5-containing epidermoid carcinoma A431 cell skeleton complex preparation, generated by washing off intracellular proteins with 1% Triton followed with 2 M urea in 1 M NaCl (22), was digested with recombinant human Cat S. Under physiological concentrations (0.15–3 nM), Cat S cleaved γ2 and produced γ2′ and γ2χ peptides (Fig. 7*C*), which can be preferentially detected by monoclonal antibody 19562 (Chemicon; see Ref. 49). Higher concentrations (60 nM) of

Cat S produced more 50-kDa γ2″ fragments. We consistently demonstrated impaired production of γ2′, γ2χ, and γ2″ peptides in Cat $S^{-/-}$ endothelial cells cultured with the same A431 cell skeleton complex preparation. The absence of Cat S in endothelial cells led to decreased γ2′ and γ2χ peptides in culture media and decreased all three (γ2′, γ2χ, and γ2″) peptides in the lysate fraction, which contains both endothelial cells and residual A431 cell skeleton proteins (Fig. 7*D*), demonstrating a novel function of Cat S in the production of pro-angiogenic γ2 fragments.

To examine whether γ2′ (100 kDa), γ2χ (80 kDa), and γ2″ (50 kDa) peptides (Fig. 7*C*) produced by Cat S are bioactive, we immunopurified these peptides from the digestion pool of various amount of recombinant Cat S with A431 cell skeleton complex preparation using an affinity gel coated with laminin-5 γ2-monoclonal antibody. Purified proteins were verified by both silver staining and immunoblot analysis with laminin-5 γ2-monoclonal antibody. We were able to purify three fractions containing the γ2′, γ2χ with γ2″, and γ2″ alone (Fig. 8*A*). Purified peptides permitted us to assess their bioactivity in promoting microvessel growth in an aortic ring assay. Consistent with earlier reports (43, 44), Cat S-produced γ2′ and γ2χ peptides, but not γ2″, showed significant activity in promoting microvessel sprouting from the aortic rings (Fig. 8*B*), providing another possible mechanistic explanation for the regulation of angiogenesis and tumor growth by Cat S *in vivo*.

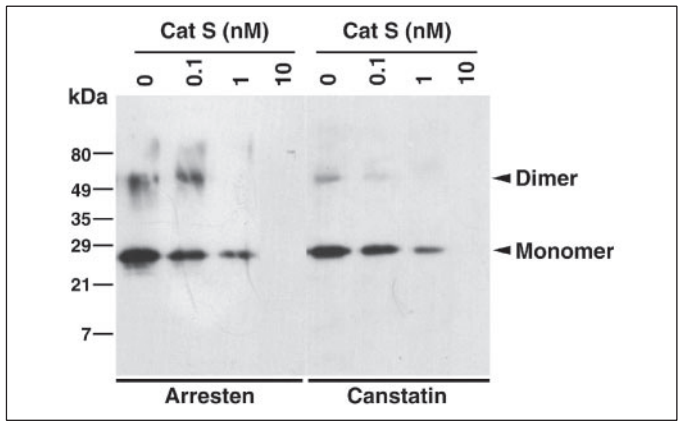

FIGURE 5. ***In vitro* digestion of murine recombinant arresten and canstatin by Cat S.** One microgram of purified arresten or canstatin was digested with various amounts of recombinant human Cat S. Both monomer (~25 kDa) and dimer (~50 kDa) of these anti-angiogenic peptides are indicated.

DISCUSSION

A role for cysteine proteases in tumor progression was proposed decades ago (50). Until recently, however, investigations have been focused on demonstrating that inhibition of cysteine protease activities affects angiogenesis and tumor invasion *in vivo* (6–8, 11) and therefore highlighted the significance of this family of proteases in tumor pathogenesis. Although we have proposed a role for cysteine protease Cat S in angiogenesis and presumably in tumor growth, we have had no direct *in vivo* evidence for or any mechanistic explanation of Cat S involvement. Several *in vitro* experiments demonstrated cysteine protease activities in the generation of anti-angiogenic endostatin (32, 33), conversion of pro-angiogenic factor TGF-β (51, 52), and activation of tumor invasion-associated urokinase-type plasminogen activator (53). It remains uncertain whether these *in vitro* activities of cysteine proteases have any pathophysiologic relevance *in vivo*.

The present study demonstrated an important role for Cat S and its endogenous inhibitor Cyst C in regulating angiogenesis and tumor growth in a genetically engineered mouse model of pancreatic islet cancer (9). By using gene knock-out mice, we have clearly demonstrated that Cat S contributes to angiogenesis and tumor progression, likely in several ways. First, Cat S regulates levels of anti-angiogenic arresten and canstatin, two degradation products of the basement membrane matrix protein type IV collagen α1 and α2 chains, respectively (16–18, 36, 37). Several *in vitro* and *in vivo* experiments demonstrated that these peptides inhibited angiogenesis and tumor progression via expression of cell-surface proteoglycan and integrins (α1β1 and αVβ3) to affect cell apoptosis (16), cell cycle protein cyclin D1, or proteases (54). For example, overexpression of canstatin in culture inhibited the migration and proliferation of endothelial cells, induced apoptosis of endothelial cells (16, 17), and suppressed murine melanoma growth *in vivo* (17). However, the proteases responsible for initial type IV collagen degradation have not been identified. In this study, we found a decreased level of these peptides whenever Cat S was expressed. Reduced expression of Cat S expression was associated with increased levels of these peptides, suggesting a participation of this protease in the degradation of anti-angiogenic peptides or inactivation of proteases responsible for the generation of such peptides. Indeed, recombinant Cat S degraded both canstatin and arresten *in vitro* under physiological concentrations. More importantly, expression of Cat S did not affect serum levels of endostatin, a well known collagen-XVIII degradation product, although many cathepsins, including Cat L and Cat S, have been shown to produce such peptides *in vitro* (32, 33). Altered expression of these cysteine proteases in the RIP1-Tag2/Cyst $C^{-/-}$ mice (Fig. 2*A*) did not affect circulating endostatin levels (Table 1). Although we cannot exclude the possibility that other cathepsins, including Cat L, regulate endostatin levels *in vivo*, Cat S is probably less important in the production or degradation of endostatin, because a lack of Cat S expression had no significant impact on endostatin levels in either sera or tumor extracts (Table 1). Second, Cat S produces the pro-angiogenic γ2 subunits γ2′ and γ2χ from the laminin-5 complex, another major component of the basement membrane matrix that plays an important role in tumor cell adhesion, migration, invasion, and metastasis. Data from experiments with cultured Cat S-deficient endothelial cells, recombinant Cat S, and Cat $S^{-/-}$ mice all supported this conclusion. Increased levels of these γ2 peptides in the RIP1-Tag2/Cyst $C^{-/-}$ mice tumor extracts, which had enhanced Cat S activity, reciprocally support a participation of Cat S in γ2 peptide production. Third, Cat S affects tumor cell proliferation, although we do not yet know the mechanism responsible for this observation. We did not detect significant changes in circulating or tumor tissue growth factors (Table 1), including VEGF, IGF, and TGF-β1. In contrast, bFGF levels in Cat $S^{-/-}$ tumor tissue extracts was even higher than those from Cat $S^{+/+}$ tumor extracts (Table 1). Therefore, additional mechanisms must be involved in the alteration of tumor cell proliferation via Cat S (Fig. 3).

The role of Cyst C in tumor growth (Fig. 1, *D–F*) or tumor cell proliferation (Fig. 3) could be more than just inhibiting cysteine protease activity, although the lack of Cyst C did increase cathepsin activity (Fig. 2*A*). For instance, RIP1-Tag2/Cyst $C^{-/-}$ mice had significantly higher tissue bFGF and serum IGF (Table 1), which may explain the increased tumor burden (Fig. 1, *D–F*) and tumor cell proliferation (Fig. 3). Such increases in mitogenic factors cannot be explained by the increase in cysteine protease activity alone. Indeed, tumor tissues from RIP1-Tag2/Cat $S^{-/-}$ mice contained more bFGF than those from RIP1-Tag2/Cat $S^{+/+}$ mice (Table 1). Therefore, additional mechanisms may be involved. For instance, Cyst C may act as an antagonist of the TGF-β receptor and therefore interfere with TGF-β signaling and further affect cancer cell growth (26, 27).

Although Cat S deficiency significantly reduced the number of pan-

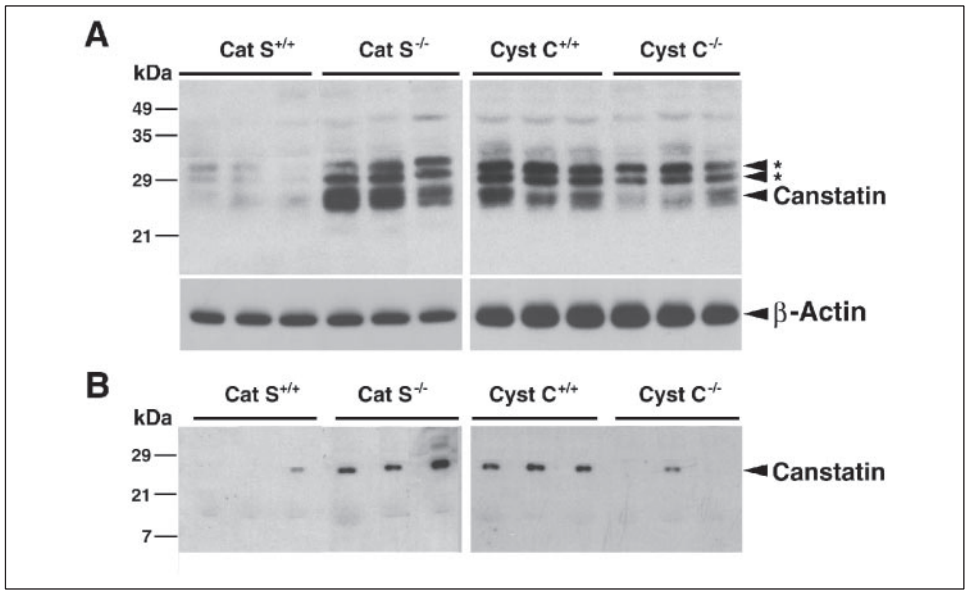

FIGURE 6. **Immunoreactive canstatins are altered in 12.5-week-old mice with deficient expression of Cat S or Cyst C.** *A,* immunoblot analysis of tissue extracts demonstrated increased canstatin in Cat $S^{-/-}$ tumors but reduced canstatin in Cyst $C^{-/-}$ tumors. Mouse β-actin immunoblot was used for protein loading control. Both β-actin and 24-kDa canstatin were indicated with *arrowheads. Two asterisks* indicate partially processed canstatin molecules. *B,* immunoblot analysis of mouse serum showed increased 24-kDa canstatin in Cat $S^{-/-}$ mice and decreased canstatin in Cyst $C^{-/-}$ mice.

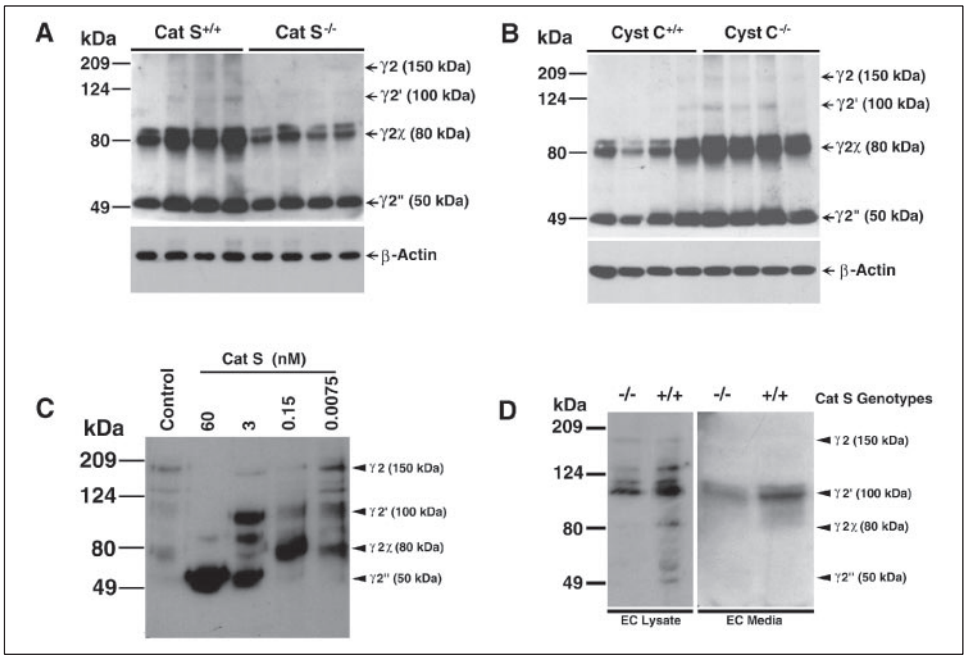

FIGURE 7. **Laminin-5 γ2 processing by Cat S.** *A,* mouse laminin-5 γ2 immunoblot analysis of RIP1-Tag2 tissue extracts from Cat $S^{+/+}$ and Cat $S^{-/-}$ mice (12.5 weeks). *B,* mouse laminin-5 γ2 immunoblot analysis of RIP1-Tag2 tissue extracts from Cyst $C^{+/+}$ and Cyst $C^{-/-}$ mice (12.5 weeks). Mouse β-actin immunoblot was performed for equal protein loadings. *C,* A431 cell skeleton preparation digestion with human recombinant Cat S followed by immunoblot analysis with human laminin-5 γ2 monoclonal antibody. *D,* A431 cell skeleton preparation digestion with live mouse endothelial cells from Cat $S^{+/+}$ and Cat $S^{-/-}$ mice. Both culture media (*right*) and cell lysates (*left*) were immunoblotted and analyzed with human laminin-5 γ2 monoclonal antibody. All γ2, γ2′, γ2χ, and γ2″ are indicated by *arrowheads.*

creatic islet cell carcinomas as well as angiogenic islets (Fig. 1), the life span of RIP1-Tag2/Cat $S^{-/-}$ mice was extended by only 2 weeks on average relative to that of RIP1-Tag2/Cat $S^{+/+}$ mice (Fig. 2). Therefore, altered angiogenesis may primarily affect tumor growth in this model, with a lesser effect on life span, which may be influenced by additional mechanisms. Many RIP1-Tag2 transgenic mice bear the phenotype of islet hyperplasia, leading to hypoglycemia, a cause of sudden death in RIP1-Tag2 transgenic mice (9). Although we detected no difference between the serum glucose levels of Cat $S^{-/-}$ mice and C57/Bl6 wild-type mice or Cyst $C^{-/-}$ mice and their wild-type littermates, all RIP1-Tag2 transgenic mice had reduced serum glucose levels (Fig. 2*C*). The serum glucose levels of most mice from the RIP1-Tag2/Cat $S^{+/+}$, RIP1-Tag2/Cyst $C^{+/+}$, and RIP1-Tag2/Cyst $C^{-/-}$ groups were ~25 mg/dl, values significantly lower than those of their nontransgenic counterparts. This is probably why we did not detect significant differences in life span between RIP1-Tag2/Cyst $C^{+/+}$ and RIP1-Tag2/Cyst $C^{-/-}$ mice, as both groups had lower serum glucose levels. In contrast, RIP1-Tag2 mice with Cat S deficiency had much higher glucose levels than their Cat $S^{+/+}$ counterparts, which could be one cause of the 2-week extension in life span of the deficient mice (Fig. 2), although such levels are still lower than those of nontransgenic counterparts. Additional sugar in the diet prolonged the life span of RIP1-Tag2 transgenic mice by up to 20 weeks (9). Therefore, Cat S deficiency impaired islet hyperplasia (Fig. 3), consequently increasing serum glucose levels (Fig. 2*C*) and ultimately prolonging life span (Fig. 2).

It remains unexplained why RIP1-Tag2/Cat $S^{+/+}$ and RIP1-Tag2/Cyst $C^{+/+}$ mice differed in their tumor sizes (Fig. 1), numbers of proliferating tumor cells (Fig. 3), tumor canstatin levels (Fig. 4*B* and Fig. 5, *A* and *B*), and even life span (13.3 ± 0.3 *versus* 15.7 ± 0.7, $p = 0.02$), although the mice were wild type for both Cat S and Cyst C. Such discrepancies could be due to their different genetic backgrounds. RIP1-Tag2/Cat $S^{+/+}$ mice were on pure C57/Bl6 background, whereas RIP1-

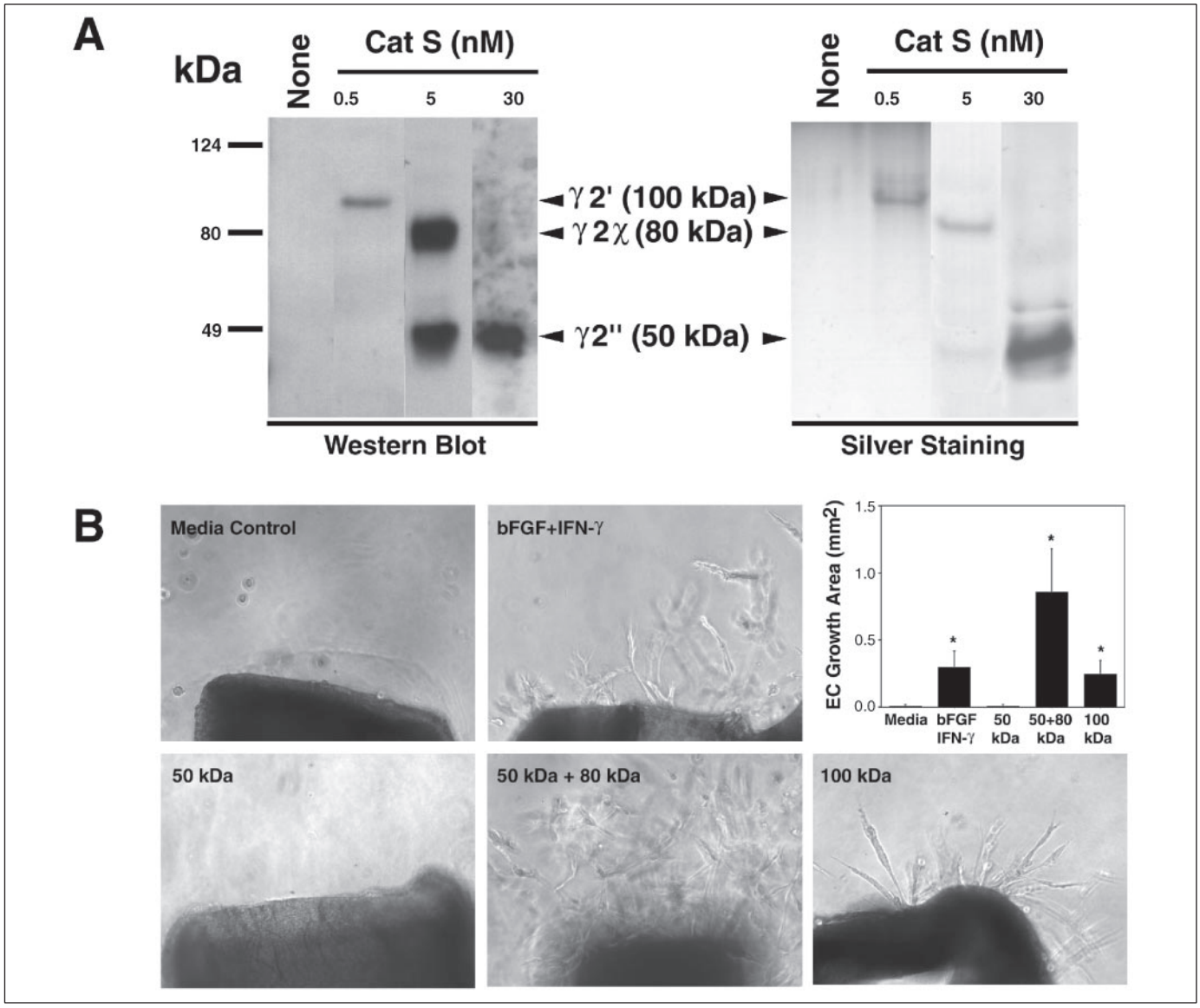

FIGURE 8. **Purification and bioactivity assay of human laminin-5 γ2 fragments.** *A,* human A431 cell skeleton preparation was digested with recombinant human Cat S at the indicated concentrations and purified over an AminoLink® Plus coupling gel coated with human laminin-5 γ2 monoclonal antibody. Each elute was analyzed by immunoblot with laminin-5 γ2 monoclonal antibody (*left panel*) and silver staining (*right panel*). *B,* aortic ring assay demonstrated the relative bioactivity of all three γ2 fragments. Among them, γ2χ had the highest potency in endothelial sprouting. Murine bFGF (10 ng/ml) and interferon-γ (500 units/ml) were used as a positive control and plain medium as negative control for the assay.

Tag2/Cyst $C^{+/+}$ mice were on C57/Bl6/129S mixed background. It has been shown that VEGF and bFGF behaved differently in mice with C57/BL6 and 129S backgrounds in inducing tumor growth or neovascularization (55, 56). Indeed, the numbers of both endothelial progenitor cells and circulating blood endothelial cells, which are subsequently incorporated into distal sites of ongoing sprouting angiogenesis, were different among various genetic backgrounds (56). Therefore, more investigations are required to reveal the factors that lead to the different phenotypes of RIP1-Tag2/Cat $S^{+/+}$ mice and RIP1-Tag2/Cyst $C^{+/+}$ mice from this study.

In conclusion, our findings support the hypothesis that Cat S is required for angiogenesis (14) and is associated with the pathobiology of tumor growth, at least in the RIP1-Tag2 model system. The reduction in tumor sizes through the inhibition of total cysteine proteases with JPM-ethyl ester (11) may also occur, at least in part, via its inhibitory effect on Cat S. Therefore, it might be possible to manage tumor growth critically dependent on angiogenesis by targeting Cat S activity.

Acknowledgments—We thank Dr. D. Hanahan (University of California, San Francisco) for the RIP1-Tag2 mice, advice during the initiation of the project, and critical comments on the manuscript. We thank Dr. Johanna Joyce (Memorial Sloan Kettering Cancer Center, New York) for assistance with the RIP1-Tag2 mice characterization. We also thank Dr. R. Timpl (Max-Planck-Institut für Biochemie, Germany) for providing the murine laminin-5 γ2 monoclonal antibodies and Dr. M. E. Hemler (Harvard University) for critical reading of the manuscript.

REFERENCES

1. Folkman, J. (1971) *N. Engl. J. Med.* **285,** 1182–1186
2. Folkman, J. (1995) *Nat. Med.* **1,** 27–31
3. Mook, O. R., Frederiks, W. M., and Van Noorden, C. J. (2004) *Biochim. Biophys. Acta* **1705,** 69–89
4. Pepper, M. S. (2001) *Thromb. Haemostasis* **86,** 346–355
5. Jedeszko, C., and Sloane, B. F. (2004) *Biol. Chem.* **385,** 1017–1027
6. Yanamandra, N., Gumidyala, K. V., Waldron, K. G., Gujrati, M., Olivero, W. C., Dinh, D. H., Rao, J. S., and Mohanam, S. (2004) *Oncogene* **23,** 2224–2230

7. Lakka, S. S., Gondi, C. S., Yanamandra, N., Olivero, W. C., Dinh, D. H., Gujrati, M., and Rao, J. S. (2004) *Oncogene* **23,** 4681–4689
8. Gondi, C. S., Lakka, S. S., Dinh, D. H., Olivero, W. C., Gujrati, M., and Rao, J. S. (2004) *Oncogene* **23,** 8486–8496
9. Bergers, G., Brekken, R., McMahon, G., Vu, T. H., Itoh, T., Tamaki, K., Tanzawa, K., Thorpe, P., Itohara, S., Werb, Z., and Hanahan, D. (2000) *Nat. Cell Biol.* **2,** 737–744
10. Meara, J. P., and Rich, D. H. (1996) *J. Med. Chem.* **39,** 3357–3366
11. Joyce, J. A., Baruch, A., Chehade, K., Meyer-Morse, N., Giraudo, E., Tsai, F. Y., Greenbaum, D. C., Hager, J. H., Bogyo, M., and Hanahan, D. (2004) *Cancer Cell* **5,** 443–453
12. Hershberg, R. M., Framson, P. E., Cho, D. H., Lee, L. Y., Kovats, S., Beitz, J., Blum, J. S., and Nepom, G. T. (1997) *J. Clin. Investig.* **100,** 204–215
13. Vigneswaran, N., Wu, J., Nagaraj, N., Adler-Storthz, K., and Zacharias, W. (2005) *Int. J. Oncol.* **26,** 103–112
14. Shi, G. P., Sukhova, G. K., Kuzuya, M., Ye, Q., Du, J., Zhang, Y., Pan, J. H., Lu, M. L., Cheng, X. W., Iguchi, A., Perrey, S., Lee, A. M., Chapman, H. A., and Libby, P. (2003) *Circ. Res.* **92,** 493–500
15. Sukhova, G. K., Wang, B., Libby, P., Pan, J. H., Zhang, Y., Grubb, A., Fang, K., Chapman, H. A., and Shi, G. P. (2005) *Circ. Res.* **96,** 368–375
16. Kamphaus, G. D., Colorado, P. C., Panka, D. J., Hopfer, H., Ramchandran, R., Torre, A., Maeshima, Y., Mier, J. W., Sukhatme, V. P., and Kalluri, R. (2000) *J. Biol. Chem.* **275,** 1209–1215
17. Colorado, P. C., Torre, A., Kamphaus, G., Maeshima, Y., Hopfer, H., Takahashi, K., Volk, R., Zamborsky, E. D., Herman, S., Sarkar, P. K., Ericksen, M. B., Dhanabal, M., Simons, M., Post, M., Kufe, D. W., Weichselbaum, R. R., Sukhatme, V. P., and Kalluri, R. (2000) *Cancer Res.* **60,** 2520–2526
18. Maeshima, Y., Manfredi, M., Reimer, C., Holthaus, K. A., Hopfer, H., Chandamuri, B. R., Kharbanda, S., and Kalluri, R. (2001) *J. Biol. Chem.* **276,** 15240–15248
19. Wild, R., Ramakrishnan, S., Sedgewick, J., and Griffioen, A. W. (2000) *Microvasc. Res.* **59,** 368–376
20. Fang, K. C., Raymond, W. W., Lazarus, S. C., and Caughey, G. H. (1996) *J. Clin. Investig.* **97,** 1589–1596
21. Sasaki, T., Gohring, W., Mann, K., Brakebusch, C., Yamada, Y., Fassler, R., and Timpl, R. (2001) *J. Mol. Biol.* **314,** 751–763
22. Weitzman, J. B., Pasqualini, R., Takada, Y., and Hemler, M. E. (1993) *J. Biol. Chem.* **268,** 8651–8657
23. Shi, G. P., Bryant, R. A., Riese, R., Verhelst, S., Driessen, C., Li, Z., Bromme, D., Ploegh, H. L., and Chapman, H. A. (2000) *J. Exp. Med.* **191,** 1177–1186
24. Kato, T., Kure, T., Chang, J. H., Gabison, E. E., Itoh, T., Itohara, S., and Azar, D. T. (2001) *FEBS Lett.* **508,** 187–190
25. Hall, A., Ekiel, I., Mason, R. W., Kasprzykowski, F., Grubb, A., and Abrahamson, M. (1998) *Biochemistry* **37,** 4071–4079
26. Sokol, J. P., and Schiemann, W. P. (2004) *Mol. Cancer Res.* **2,** 183–195
27. Sokol, J. P., Neil, J. R., Schiemann, B. J., and Schiemann, W. P. (2005) *Breast Cancer Res.* **7,** R844–R853
28. Lee, C. Y., and Rechler, M. M. (1996) *Endocrinology* **137,** 2051–2058
29. Fowlkes, J. L., and Winkler, M. K. (2002) *Cytokine Growth Factor Rev.* **13,** 277–287
30. Buczek-Thomas, J. A., Lucey, E. C., Stone, P. J., Chu, C. L., Rich, C. B., Carreras, I., Goldstein, R. H., Foster, J. A., and Nugent, M. A. (2004) *Am. J. Respir. Cell Mol. Biol.* **31,** 344–350
31. Martineau, I., Lacoste, E., and Gagnon, G. (2004) *Biomaterials* **25,** 4489–4502
32. Felbor, U., Dreier, L., Bryant, R. A., Ploegh, H. L., Olsen, B. R., and Mothes, W. (2000) *EMBO J.* **19,** 1187–1194
33. Ferreras, M., Felbor, U., Lenhard, T., Olsen, B. R., and Delaisse, J. (2000) *FEBS Lett.* **486,** 247–251
34. Wen, W., Moses, M. A., Wiederschain, D., Arbiser, J. L., and Folkman, J. (1999) *Cancer Res.* **59,** 6052–6056
35. Lin, H. C., Chang, J. H., Jain, S., Gabison, E. E., Kure, T., Kato, T., Fukai, N., and Azar, D. T. (2001) *Investig. Ophthalmol. Vis. Sci.* **42,** 2517–2524
36. Maeshima, Y., Yerramalla, U. L., Dhanabal, M., Holthaus, K. A., Barbashov, S., Kharbanda, S., Reimer, C., Manfredi, M., Dickerson, W. M., and Kalluri, R. (2001) *J. Biol. Chem.* **276,** 31959–31968
37. He, G. A., Luo, J. X., Zhang, T. Y., Wang, F. Y., and Li, R. F. (2003) *Biochem. Biophys. Res. Commun.* **312,** 801–805
38. Hamano, Y., Zeisberg, M., Sugimoto, H., Lively, J. C., Maeshima, Y., Yang, C., Hynes, R. O., Werb, Z., Sudhakar, A., and Kalluri, R. (2003) *Cancer Cell* **3,** 589–601
39. Liu, J., Ma, L., Yang, J., Ren, A., Sun, Z., Yan, G., Sun, J., Fu, H., Xu, W., Hu, C., and Shi, G. P. (2006) *Atherosclerosis,* in press
40. Martin, K. J., Kwan, C. P., Nagasaki, K., Zhang, X., O'Hare, M. J., Kaelin, C. M., Burgeson, R. E., Pardee, A. B., and Sager, R. (1998) *Mol. Med.* **4,** 602–613
41. Gonzales, M., Haan, K., Baker, S. E., Fitchmun, M., Todorov, I., Weitzman, S., and Jones, J. C. (1999) *Mol. Biol. Cell* **10,** 259–270
42. Lohi, J. (2001) *Int. J. Cancer* **94,** 763–767
43. Seftor, R. E., Seftor, E. A., Koshikawa, N., Meltzer, P. S., Gardner, L. M., Bilban, M., Stetler-Stevenson, W. G., Quaranta, V., and Hendrix, M. J. (2001) *Cancer Res.* **61,** 6322–6327
44. Zent, R., Bush, K. T., Pohl, M. L., Quaranta, V., Koshikawa, N., Wang, Z., Kreidberg, J. A., Sakurai, H., Stuart, R. O., and Nigam, S. K. (2001) *Dev. Biol.* **238,** 289–302
45. Marinkovich, M. P., Lunstrum, G. P., and Burgeson, R. E. (1992) *J. Biol. Chem.* **267,** 17900–17906
46. Giannelli, G., Falk-Marzillier, J., Schiraldi, O., Stetler-Stevenson, W. G., and Quaranta, V. (1997) *Science* **277,** 225–228
47. Amano, S., Scott, I. C., Takahara, K., Koch, M., Champliaud, M. F., Gerecke, D. R., Keene, D. R., Hudson, D. L., Nishiyama, T., Lee, S., Greenspan, D. S., and Burgeson, R. E. (2000) *J. Biol. Chem.* **275,** 22728–22735
48. Koshikawa, N., Schenk, S., Moeckel, G., Sharabi, A., Miyazaki, K., Gardner, H., Zent, R., and Quaranta, V. (2004) *FASEB J.* **18,** 364–366
49. Siler, U., Rousselle, P., Muller, C. A., and Klein, G. (2002) *Br. J. Haematol.* **119,** 212–220
50. Sloane, B. F., Dunn, J. R., and Honn, K. V. (1981) *Science* **212,** 1151–1153
51. Guo, M., Mathieu, P. A., Linebaugh, B., Sloane, B. F., and Reiners, J. J. (2002) *J. Biol. Chem.* **277,** 14829–14837
52. Somanna, A., Mundodi, V., and Gedamu, L. (2002) *J. Biol. Chem.* **277,** 25305–25312
53. Kobayashi, H., Schmitt, M., Goretzki, L., Chucholowski, N., Calvete, J., Kramer, M., Gunzler, W. A., Janicke, F., and Graeff, H. (1991) *J. Biol. Chem.* **266,** 5147–5252
54. Pasco, S., Ramont, L., Venteo, L., Pluot, M., Maquart, F. X., and Monboisse, J. C. (2004) *Exp. Cell Res.* **301,** 251–265
55. Rohan, R. M., Fernandez, A., Udagawa, T., Yuan, J., and D'Amato, R. J. (2000) *FASEB J.* **14,** 871–876
56. Shaked, Y., Bertolini, F., Man, S., Rogers, M. S., Cervi, D., Foutz, T., Rawn, K., Voskas, D., Dumont, D. J., Ben-David, Y., Lawler, J., Henkin, J., Huber, J., Hicklin, D. J., D'Amato, R. J., and Kerbel, R. S. (2005) *Cancer Cell* **7,** 101–111

Cathepsin S Controls Angiogenesis and Tumor Growth via Matrix-derived Angiogenic Factors

Bing Wang, Jiusong Sun, Shiro Kitamoto, Min Yang, Anders Grubb, Harold A. Chapman, Raghu Kalluri and Guo-Ping Shi

J. Biol. Chem. 2006, 281:6020-6029.
doi: 10.1074/jbc.M509134200 originally published online December 19, 2005
